The American Journal of Pathology, Vol. 170, No. 3, March 2007

DOI: 10.2353/ajpath.2007.060031

Tumorigenesis and Neoplastic Progression

Human Breast Fibroblasts Inhibit Growth of the MCF10AT Xenograft Model of Proliferative Breast Disease

Andrea Sadlonova,* Shibani Mukherjee,* Damon B. Bowe,† Sandra R. Gault,* Nicole A. Dumas,‡ Brian A. Van Tine,* Natalya Frolova,* Grier P. Page,§ Danny R. Welch,* Lea Novak,* and Andra R. Frost*

From the Departments of Pathology, Medicine,† Pharmacology and Toxicology,‡ and Biostatistics,§ The University of Alabama at Birmingham, Birmingham, Alabama*

Stromal fibroblasts are important for normal breast homeostasis and regulation of epithelial growth; however, this regulatory function is altered during carcinogenesis. To study the role of fibroblasts in the development of breast cancer, fibroblasts derived from normal breast (NAFs) were incorporated into the MCF10AT xenograft model of progressive proliferative breast disease. The persistence of human NAFs in xenografts was established by intracellular labeling and tyramide-coupled fluorescent *in situ* hybridization. Overall, the number of MCF10AT epithelial structures was decreased, and the rate of epithelial cell apoptosis was increased in xenografts containing NAFs. However, these changes were primarily in low-grade epithelial structures, corresponding to normal or mildly hyperplastic ductal epithelium. The level and rate of apoptosis of high-grade epithelial structures, corresponding to *in situ* and invasive carcinoma, were not consistently altered by NAFs. In addition, there was variability in the growth-inhibitory capacity of NAFs derived from different individuals. NAFs induced changes in the morphology of high-grade MCF10AT structures and in xenograft stroma, including the composition of extracellular matrix, and increased angiogenesis and lymphocytic infiltration. These findings imply that NAFs can inhibit the growth of normal and hyperplastic epithelium but are less able to regulate the more transformed epithelial cells that arise during carcinogenesis. *(Am J Pathol 2007, 170:1064–1076; DOI: 10.2353/ajpath.2007.060031)*

During breast carcinogenesis, concurrent morphological and molecular changes occur in stromal and epithelial compartments.[1–3] The genetic and phenotypic transformation of epithelial cells in cancer is accompanied by activation of adjacent stroma, which can support cancer development and progression. The stroma surrounding benign and malignant breast epithelium consists of extracellular matrix (ECM) and cellular components, including fibroblasts, adipocytes, blood vessels, and immune and inflammatory cells, all of which have the potential to influence carcinogenesis.[4–6] To study the stromal-epithelial interactions in cancer, xenograft models have evolved to incorporate the human stromal component, fibroblasts in particular, and examine their effect on the tumorigenic process.[7]

Fibroblasts surrounding and within invasive breast carcinomas [ie, carcinoma-associated fibroblasts (CAFs)] are genotypically, phenotypically, and functionally distinct from the fibroblasts of the normal breast [ie, normal breast-associated fibroblasts (NAFs)].[1,2,5,8–12] A subset of the genotypic and phenotypic alterations characteristic of CAFs has been documented in stroma surrounding *in situ* breast lesions, including atypical hyperplasia and ductal carcinoma *in situ*.[8–10,13–16]

We have previously shown that NAFs and CAFs differ in their ability to inhibit the growth of MCF10A and MCF10AT breast epithelial cell lines, which are representative of low-risk and high-risk proliferative breast disease, respectively.[17–20] In co-culture *in vitro*, NAFs suppressed the growth of both MCF10A and MCF10AT; however, CAFs inhibited only MCF10A and not the more transformed MCF10AT cells, suggesting that CAFs had less growth-inhibitory capacity than NAFs.[12] Interest-

Supported by the National Institutes of Health (grants CA097472 and CA105950) and the National Foundation for Cancer Research.

Accepted for publication November 28, 2006.

A guest editor acted as editor-in-chief for this manuscript. No person at the University of Alabama at Birmingham was involved in the peer review process or final disposition for this article.

Address reprint requests to Andra R. Frost, Department of Pathology, The University of Alabama at Birmingham, WTI 420, 1824 6th Ave. South, Birmingham, AL 35294. E-mail: afrost@uab.edu.

ingly, another study reported that CAFs promoted the growth of both of these epithelial cell lines *in vitro*.[21]

In the present study, incorporation of NAFs into the MCF10AT xenograft model allowed examination of the role of fibroblasts in the development and progression of *in situ* proliferative breast lesions to invasive carcinoma. The MCF10AT cell line was developed from MCF10A cells, a spontaneously immortalized cell line originally derived from benign proliferative breast disease, by transfection of a mutated, constitutively activated T24 H-ras oncogene. When suspended in Matrigel and grown as xenografts in immunodeficient nude or nude/beige mice, MCF10AT cells form structures that resemble normal human breast ducts or lobular acini, ductal hyperplasias of varying degrees of severity, and/or *in situ* carcinomas. A subset of xenografts develop lesions resembling invasive carcinoma.[18–20] The presence and persistence of human NAFs in xenografts was confirmed by labeling with a fluorescent green tracker and by tyramide fluorescent *in situ* hybridization (T-FISH) with a probe specific for human DNA. The effect of NAFs on the growth of MCF10AT lesions and xenograft stroma was assessed.

Materials and Methods

Maintenance of MCF10AT Cells

MCF10AT cells (Karmanos Cancer Institute, Detroit, MI) were cultivated in Dulbecco's modified Eagle's medium/Ham's F-12 (with L-glutamine, 15 mmol/L 4-(2-hydroxyethyl)-1-piperazineethanesulfonic acid (HEPES), sodium pyruvate; BioWhittaker Cambrex, Walkersville, MD) supplemented with 0.1 μg/ml cholera toxin (Calbiochem, San Diego, CA), 10 μg/ml insulin (Sigma, St. Louis, MO), 0.5 μg/ml hydrocortisone (Sigma), 0.02 μg/ml epidermal growth factor (Upstate Biotechnology, Lake Placid, NY), and 5% horse serum (Invitrogen, Carlsbad, CA) in a humidified, 5% CO_2, 37°C incubator.

Isolation, Characterization, and Maintenance of Fibroblast Cultures

Fibroblast cultures (NAF1, NAF2, NAF3) were isolated from breast reduction specimens from three different women. The specimens were obtained via the University of Alabama at Birmingham Tissue Procurement Facility after institutional review board approval. For fibroblast isolation, the breast tissue was digested with 150 U/ml hyaluronidase (Sigma) and 200 U/ml collagenase type III (Life Technologies, Grand Island, NY) for 18 to 24 hours at 37°C. The digested tissue was centrifuged at 100 $\times$ *g* and the supernatant plated in 25-cm^2 tissue culture flasks with 10% fetal bovine serum (Hyclone, Logan, UT) in Dulbecco's modified Eagle's medium (with 1 g/L glucose, L-glutamine, sodium pyruvate; Cellgro Mediatech, Inc., Herndon, VA). During subculturing, differential trypsinization was used to select for the growth of primary fibroblasts.[12] The isolated fibroblasts were maintained in Dulbecco's modified Eagle's medium and 10% fetal bovine serum.

To exclude epithelial cell contamination of fibroblast cultures, immunocytochemical evaluation for epithelial membrane antigen (EMA, 1.06 μg/ml dilution, mouse IgG2a, clone ZCE113; Zymed, San Francisco, CA) and cytokeratin (CK) 5/8 (0.167 μg/ml dilution, mouse IgG_1, clone C-50; Neomarkers, Fremont, CA), both epithelial markers, was negative. Immunocytochemistry for vimentin, a stromal cell marker (0.5 μg/ml dilution, mouse IgG_1, clone V9; Neomarkers) was positive. Secondary detection was performed as described below for immunohistochemistry.

Establishment of MCF10AT Xenografts, NAF Xenografts, and MCF10AT + NAF Xenografts

MCF10AT xenografts and normal breast fibroblast (NAF) xenografts consisted of 5×10^6 of each respective cell type. MCF10AT + NAF xenografts consisted of MCF10AT epithelial cells admixed with one of three NAF cultures (NAF1, NAF2, or NAF3). Each MCF10AT + NAF xenograft contained 5×10^6 MCF10AT epithelial cells and 5×10^6 NAFs. An equal amount of MCF10AT cells in MCF10AT xenografts and MCF10AT + NAF xenografts was selected so that the rate of growth and progression of the epithelial cells could be compared between the two groups. NAF1, NAF2, and NAF3 used were below passage nine. Cells for each xenograft were suspended in 230 μl of Matrigel (BD Biosciences, Franklin Lakes, NJ) and injected subcutaneously into the flanks of female CD1/nude mice (Charles River Laboratories, Wilmington, MA) at 4 to 6 weeks of age. The subcutaneous location was used to eliminate the influence of other mammary gland cellular components on the interaction of human breast fibroblasts and epithelial cells. For comparison with the subcutaneous site, MCF10A xenografts and MCF10AT + NAF xenografts were also placed in the mammary fat pad. The animals were handled in accordance with National Institutes of Health guidelines and Institutional Animal Care and Use Committee regulations. Two xenografts of the same type were injected per mouse. NAF xenografts and MCF10AT + NAF xenografts were removed at 3, 6, 12, and 20 weeks. MCF10AT xenografts were removed at 6 and 12 weeks. After removal, xenografts were immediately fixed in 4% paraformaldehyde and processed to paraffin. Histological sections, 5 μm in thickness, were prepared for histological evaluation, immunohistochemistry, and genomic tyramide fluorescent *in situ* hybridization (T-FISH).

Identification of Human NAFs in Xenografts by 5-Chloromethylfluorescein Diacetate (CMFDA) Labeling

Labeling of NAFs with CellTracker Green CMFDA Molecular Probes, Eugene, OR) for *in vitro* and *in vivo* purposes followed the manufacturer's protocol. In brief, trypsinized and pelleted fibroblasts were incubated with 5 ml of Dulbecco's modified Eagle's medium containing 10 μmol/L CMFDA for 45 minutes at 37°C in 5% CO_2. For *in*

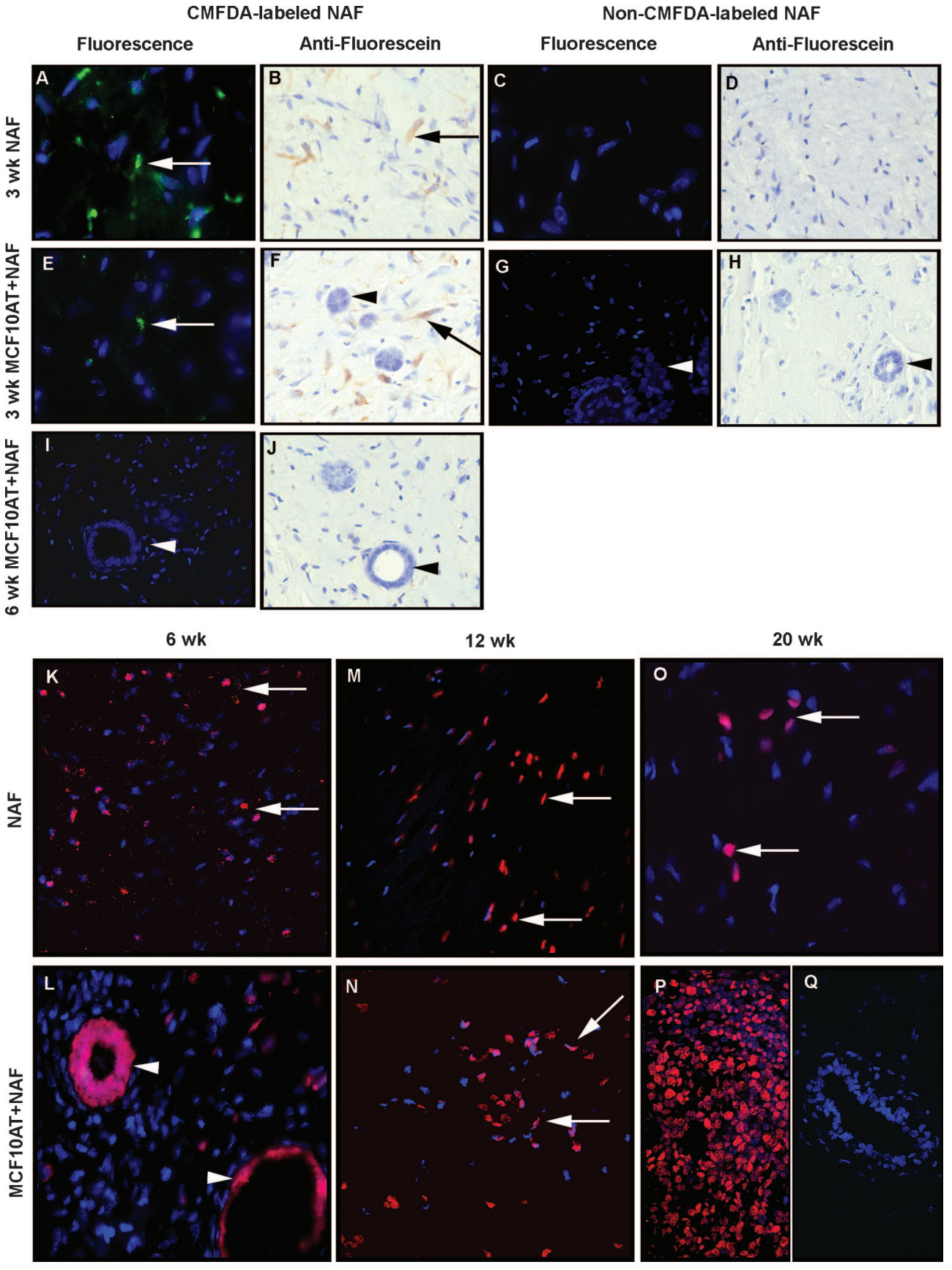
CMFDA-labeled NAF
Non-CMFDA-labeled NAF
Fluorescence
Anti-Fluorescein
Fluorescence
Anti-Fluorescein
3 wk NAF
3 wk MCF10AT+NAF
6 wk MCF10AT+NAF
A
B
C
D
E
F
G
H
I
J
6 wk
12 wk
20 wk
NAF
MCF10AT+NAF
K
M
O
L
N
P
Q

vitro study, the labeled cells were plated in 75-cm^2 tissue culture flasks. Initial fluorescence capacity of CMFDA was assessed 1 day after labeling. In addition, fluorescence capacity was assessed after subculturing labeled fibroblasts throughout a period of 6 weeks. A negative control consisted of unlabeled fibroblasts. For *in vivo* study, the labeled cells were washed with Dulbecco's modified Eagle's medium (37°C) before inoculation. Four NAF xenografts and four MCF10AT + NAF xenografts were prepared with labeled fibroblasts.

Immunohistochemistry

Xenografts containing CMFDA-labeled fibroblasts were immunostained with anti-fluorescein/Oregon Green (mouse monoclonal antibody, clone 4-4-20; Molecular Probes), which recognizes CMFDA. In brief, sections were incubated in 3% hydrogen peroxide for 5 minutes and blocked with M.O.M. Mouse IgG blocking reagent (M.O.M. Immunodetection Kit; Vector Laboratories Inc., Burlingame, CA) for 60 minutes at room temperature, followed by 20 μg/ml anti-fluorescein antibody in M.O.M. diluent for 60 minutes. A streptavidin/peroxidase secondary detection system (Multispecies USA-Biotin and USA-HRP reagents; Signet Laboratories, Dedham, MA) was used with diaminobenzidine (BioGenex, San Ramon, CA) as the chromogen. Slides were counterstained with Harris hematoxylin. Negative controls consisted of histological sections of each xenograft, which were incubated either with M.O.M. diluent or DAKO Mouse Universal Negative Control N1698 (DakoCytomation, Glostrup, Denmark) rather than the primary antibody.

Immunohistochemistry for B220/CD45R (rat IgG2, clone RA3-6B2, 0.625 μg/ml; Pharmingen BD Biosciences, San Jose, CA), CD3/HRP (rabbit polyclonal, ready-to-use antibody; DakoCytomation, Carpinteria, CA), E-cadherin (mouse IgG$_1$, clone G-10, 8 μg/ml; Santa Cruz Biotechnology, Santa Cruz, CA), fibulin 1 (mouse anti-human IgG2, clone B-5, 2 μg/ml; Santa Cruz Biotechnology), Ki67 antigen (mouse IgG1, 0.1 μg/ml; BioGenex), vimentin (mouse anti-human IgG1, clone V9, 0.08 μg/ml; Novocastra, Newcastle on Tyne, UK), von Willebrand factor (rabbit polyclonal, 6.6 μg/ml; Chemicon International, Temecula, CA), and cleaved caspase-3 (rabbit polyclonal, 1:200 dilution; Cell Signaling Technology, Danvers, MA) was performed as described above except rabbit primary antibodies were detected with a rabbit-specific secondary detection system (rabbit USA-Biotin and USA-HRP reagents; Signet Laboratories). Immunohistochemistry with anti-E-cadherin, anti-Ki67, anti-vimentin, anti-von Willebrand factor, and anti-cleaved caspase 3 required antigen retrieval, consisting of incubation in boiling 10 mmol/L citric acid monohydrate, pH 6.0 (for anti-E-cadherin, anti-Ki67, anti-vimentin, anti-von Willebrand factor) or 10 mmol/L ethylenediaminetetraacetic acid, pH 8.0 (for anti-cleaved caspase 3) for 5 minutes in a microwave oven. Immunohistochemistry with anti-CD3/HRP required proteolytic digestion with 15 μg/ml proteinase K for 5 minutes at room temperature.

Histological Assessment

Paraffin blocks containing xenografts with CMFDA-labeled fibroblasts were protected from light. For evaluation of fluorescence of CMFDA, histological sections were stained with Hoechst 33258 trihydrochloride (Bis-benzimide, 0.02 mg/ml in phosphate-buffered saline; Sigma) and viewed under fluorescence microscopy. The histological grade and number of epithelial structures in MCF10AT and MCF10AT + NAF xenografts were assessed by microscopic evaluation of the largest complete cross-section of each xenograft, determined after near complete sectioning (~20 histological sections per xenograft taken at multiple depths) and histological evaluation of xenografts. The amount of lymphocytic infiltrate was categorized on the same histological section. Ki-67- and cleaved caspase 3-positive MCF10AT cells were counted in grade 0 to 1 and grade 4 to 5 structures (all such structures present or sufficient structures to provide a maximum of 1000 MCF10AT cells) on complete cross-sections of each xenograft. Microvessel density (MVD) was assessed by counting the number of vessel cross-sections staining positively with anti-von Willebrand factor in three ×200 microscopic fields located in the areas of highest staining (hot spots) similar to the method previously described.[22]

Expression of E-cadherin, and vimentin was assessed independently in a semiquantitative manner by two of the authors (A.S., A.R.F.), and the average of the two scores was used for analysis. The intensity of immunostaining of individual cells was scored from 0 (no staining) to 4+ (strong staining), and the percentage of cells staining at each intensity was estimated. The percentage of cells at each intensity was multiplied by the corresponding intensity value, and those products were summed to obtain an immunoscore.[23,24]

Human-Specific Genomic Hybridization by T-FISH

A biotin-labeled probe specific for human DNA was prepared by nick translation (Biotin-Nick Translation Mix;

Figure 1. Detection of human NAFs labeled with CMFDA and using human-specific T-FISH in xenografts. **A–J:** The CMFDA-labeled fibroblasts (**arrows**) were detected by fluorescence microscopy (green) in NAF xenografts (**A**) and MCF10AT + NAF xenografts (**E**) at 3 weeks. These fibroblasts stained positively with anti-fluorescein antibody (brown) in both NAF xenografts (**B**) and MCF10AT + NAF xenografts (**F**) at 3 weeks. No fluorescence or positivity for the antibody was detected in fibroblasts without CMFDA labeling in NAF xenografts (**C**, **D**) and MCF10AT + NAF xenografts (**G**, **H**) at 3 weeks. No CMFDA was detected in xenografts with CMFDA-labeled fibroblasts at 6 weeks (**I**, **J**) or longer. **K–Q:** Human fibroblasts are identified by T-FISH (red nuclei) in NAF xenografts at 6 (**K**), 12 (**M**), and 20 (**O**) weeks. Murine stromal cells that spontaneously infiltrated the xenograft were not labeled by T-FISH and are, therefore, blue (Hoechst staining only). At 6 weeks, human fibroblasts (red nuclei, **arrows**) were readily located within stroma of MCF10AT + NAF xenografts (**L**) and were found both adjacent to and more distant from MCF10AT structures (**arrowhead**). In MCF10AT + NAF xenografts at 12 weeks (**N**), human fibroblasts (red nuclei, **arrows**) were diminished in number and were found primarily at a distance from MCF10AT cells. No fibroblasts or MCF10AT cells were detected in MCF10AT + NAF xenografts at 20 weeks (not shown). Positive control (**P**) consisted of human lymph node and negative control (**Q**) consisted of mouse mammary gland. **Arrowheads** mark MCF10AT cells and **arrows** indicate NAF. Original magnifications: ×400 (**A–N**, **P**, **Q**); ×1000 (**O**).

Table 1. Detection of Human NAF in NAF Xenografts and MCF10AT + NAF Xenografts

Xenograft incubation	Intracellular detection of CMFDA-labeled NAF				All NAF	
	Fluorescence microscopy		Anti-fluorescein IHC		Genomic T-FISH	
	NAF	NAF + MCF10AT	NAF	NAF + MCF10AT	NAF	NAF + MCF10AT
3 weeks	+	+	+	+	+	+
6 weeks	−	−	−	−	+	+
12 weeks	−	−	−	−	+	+
20 weeks	−	−	−	−	+	−

Roche Applied Science, Penzberg, Germany) of human cot-1 DNA (Invitrogen), which is DNA containing highly repetitive sequences, as per the manufacturer's protocol. Probe size ranged between 200 and 500 bp. Before hybridization, tissues were pretreated with 3% H_2O_2 (5 minutes, room temperature), 100 μg/ml RNase [in 2× standard saline citrate (SSC), 1 hour, 37°C], 500 μg/ml pepsin (in 200 mmol/L HCl, 30 minutes, 37°C) and denaturated in 70% formamide in 2× SSC (pH 7.0, 2 minutes, 74°C). Biotinylated probe at a concentration of 20 ng/μl was denatured at 74°C for 10 minutes and then applied on xenograft tissue sections for overnight hybridization (37°C). Application of streptavidin-linked horseradish peroxidase and cyanine 3-tyramide followed the manufacture's protocol (tyramide signal amplification fluorescence systems; NEN Life Sciences/Perkin Elmer, Boston, MA). Streptavidin was applied on tissues for 2 hours at 37°C, followed by deposition of cyanine 3-tyramide for 10 minutes at room temperature. Sections were counterstained with Hoechst 33258 for 5 minutes and mounted in anti-fade medium (0.2% *N*-propyl gallate; Sigma). Slides were viewed with confocal and regular fluorescence light microscopy.

Statistical Analysis

Differences between the numbers of epithelial structures, rates of proliferation and apoptosis, MVD, and immunoscores were assessed by Student's *t*-test, assuming unequal variance. Significance was defined as $P < 0.05$.

Results

The epithelial cells in MCF10AT xenografts consistently clustered into characteristic structures resembling ducts, acini, or epithelial proliferative lesions of the human breast; therefore, their morphological identification in xenografts was straightforward. In contrast, distinction of human from murine fibroblasts was difficult because they are morphologically similar. Murine fibroblasts were attracted to and spontaneously infiltrated to the xenografts. To confirm the presence of human NAFs in MCF10AT + NAF xenografts and NAF xenografts, CMFDA tracker and T-FISH were used.

CMFDA Tracker Persists in Fibroblasts in Vitro *for 6 Weeks and* in Vivo *for 3 Weeks*

CMFDA is a fluorescent lipophilic compound that diffuses freely into cells. Once inside the cell, the compound is conjugated with glutathione by glutathione *S*-transferase, rendering the CMFDA cell membrane impermeable.[25] *In vitro* study confirmed that 10 μmol/L CMFDA strongly labeled more than 95% of the cells and was not cytotoxic to fibroblasts. Although markedly diminished, the fluorescence capacity of the intracellular CMFDA persisted in fibroblasts that were subcultured for 6 weeks (five passages).

In vivo, the persistence of the CMFDA tracker in NAF xenografts and MCF10AT + NAF xenografts was evaluated by fluorescence microscopy and anti-fluorescein immunohistochemical staining. The CMFDA tracker survived formaldehyde fixation and was readily identified in the cytoplasm of human fibroblasts in both NAF xenografts and MCF10AT + NAF xenografts by fluorescence microscopy at 3 weeks (Figure 1, A and E). CMFDA was also detected in the fibroblast cytoplasm by anti-fluorescein staining at 3 weeks (Figure 1, B and F). At 6, 12, and 20 weeks, no fluorescence or anti-fluorescein staining was identified intracellularly in CMFDA-labeled NAF (Figure 1, I and J; Table 1).

Genomic T-FISH Confirmed the Persistence of Human Fibroblasts in Vivo *for 20 Weeks*

To identify human NAFs after 3 weeks *in vivo*, human cot-1 was labeled with cyanine 3-tyramide directing the red fluorescent signal into human nuclei and marking any human cells present in xenografts. Using this approach, the presence of human fibroblasts was confirmed in NAF xenografts, both CMFDA-labeled and non-CMFDA-labeled, at all time points examined: 3, 6, 12, and 20 weeks (Figure 1, K, M, and O; Table 1). CMFDA-labeled and unlabeled NAFs in MCF10AT + NAF xenografts were identified at 3, 6, and 12 weeks (Figure 1, L and N; Table 1). At 20 weeks, no fibroblasts were detected in MCF10AT + NAF xenografts (Table 1). The MCF10AT cells were also labeled by T-FISH but were easily distinguished from NAFs by their characteristic morphology as epithelial structures (Figure 1L).

Table 2. Adaptation of the Histological Classification of MCF10AT Structures by Dawson and Colleagues[19]

Histological grade	Classification	Description
0	Simple epithelium	1) Small ducts 2) Single layer of luminal epithelium 3) No nuclear enlargement
1	Mild hyperplasia	1) Small ducts 2) Two or three layers of epithelial cells 3) No significant luminal bridging
2	Moderate hyperplasia	1) Four or more layers of epithelial cells 2) Irregular papillary proliferation 3) Luminal bridging by nonuniform cells 4) Irregularly shaped lumens
3	Atypical hyperplasia	1) Regular micropapillary configuration 2) Marked cellular proliferation often forming luminal mass 3) Some regularity (roundness) of spaces
4	Carcinoma *in situ*	1) Distended ducts filled with cells 2) Rigid intraluminal bridges forming round spaces 3) Enlarged nuclei 4) Prominent nucleoli
5	Invasive carcinoma	1) Expanded, irregular groups of invasive cells 2) Enlarged nuclei 3) Prominent nucleoli 4) Glandular, squamous, or undifferentiated

Histological Classification of MCF10AT Cells in Xenografts

MCF10AT xenografts and MCF10AT + NAF xenografts contained epithelial structures that histologically resemble normal breast ducts and ductal epithelial lesions ranging from mild hyperplasia to invasive carcinoma. These epithelial structures were graded from 0 to 5 according to the histological classification of Dawson and colleagues[19] (Table 2). All histological grades were observed in MCF10AT and MCF10AT + NAF xenografts. For analysis, the histological grades were grouped as 0 to 1, 2 to 3, and 4 to 5.

The Number of Epithelial Structures in MCF10AT + NAF Xenografts Is Decreased

An epithelial structure was defined as a contiguous grouping of MCF10AT cells, and each structure was counted and assigned a histological grade, as depicted in Figure 2, A–C. At 6 weeks, subcutaneous MCF10AT + NAF xenografts (n = 22, mean = 194) demonstrated a significant decrease in the mean number of epithelial structures in the largest complete cross-section of each xenograft compared with MCF10AT xenografts (n = 21, mean = 412) (P = 0.002) (Figure 2D). When compared by the histological grades of individual structures, this decrease was seen only in grade 0 to 1 structures (MCF10AT, mean = 402 versus MCF10AT + NAF, mean = 182, P value = 0.001). There was no difference in the number of MCF10AT epithelial structures or the distribution of histological grades of structures in MCF10AT + NAF xenografts with CMFDA-labeled versus unlabeled NAF.

All MCF10AT xenografts contained grade 0 to 1 structures; however, 3 of 22 (14%) MCF10AT + NAF xenografts contained no grade 0 to 1 structures. Of these three xenografts, two contained no epithelial cells, and the third contained only a grade 4 to 5 structure. There was no difference in the number of MCF10AT xenografts versus MCF10AT + NAF xenografts containing grade 4 to 5 structures (62 versus 59%, respectively). However, the number of MCF10AT + NAF xenografts containing grade 2 to 3 structures (68%) was lower than MCF10AT xenografts (100%) (data not shown).

NAFs from three different individuals (NAF1, NAF2, and NAF3) were used in MCF10AT + NAF xenografts. NAFs from different individuals demonstrated variability in their capacity to decrease the number of MCF10AT structures. MCF10AT + NAF xenografts containing NAF1, NAF2, or NAF3 exhibited a 1.3- to 4.8-fold decrease in the total number of epithelial structures of all grades and in the number of grade 0 to 1 structures compared with MCF10AT xenografts (Table 3). MCF10AT xenografts containing NAF1 (MCF10AT + NAF1 xenografts) had fewer grade 0 to 1 and grade 2 to 3 structures. Although the number of grade 4 to 5 MCF10AT structures was not decreased in these xenografts, the mean size of grade 5 structures, corresponding to invasive carcinomas, was marginally decreased (mean maximal diameter was 0.7 mm in MCF10AT + NAF1 versus 1.2 mm in MCF10AT xenografts, P = 0.09). In MCF10AT xenografts containing NAF3 (MCF10AT + NAF3 xenografts), the number of grade 0 to 1 and grade 4 to 5 structures was significantly decreased. Notably, there were no grade 4 to 5 structures in MCF10AT + NAF3 xenografts. In MCF10AT xenografts containing NAF2 (MCF10AT +

NAF2 xenografts), NAF2 had little effect on the number of MCF10AT structures, inducing only a minimal decrease in grade 0 to 1 structures, which was not statistically significant. Therefore, NAF1 and NAF3 had the most growth inhibitory potential, with NAF1 reducing primarily the number of lower grade epithelial structures and NAF3 reducing both high- and low-grade structures (Table 3).

To determine whether the changes in the number of high- and low-grade MCF10AT structures induced by NAFs was accompanied by corresponding changes in proliferation and apoptosis, immunohistochemical stain-

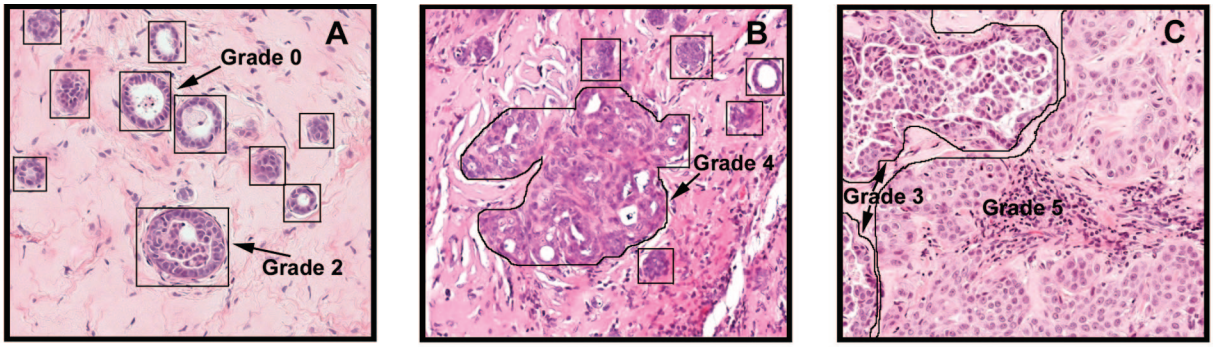

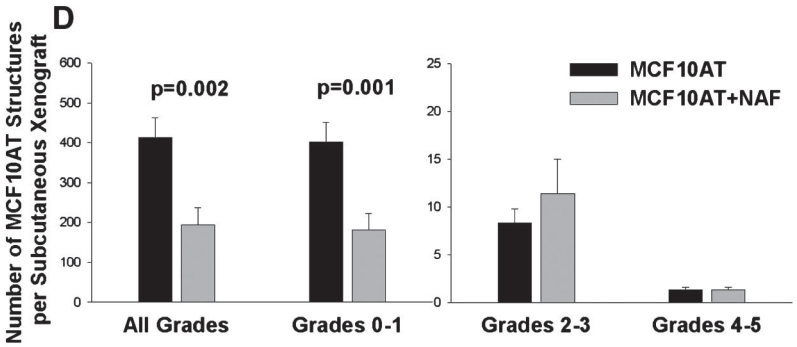

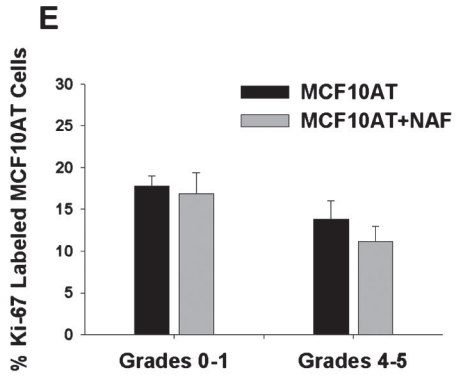

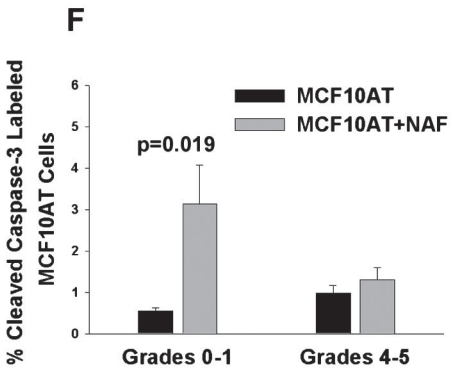

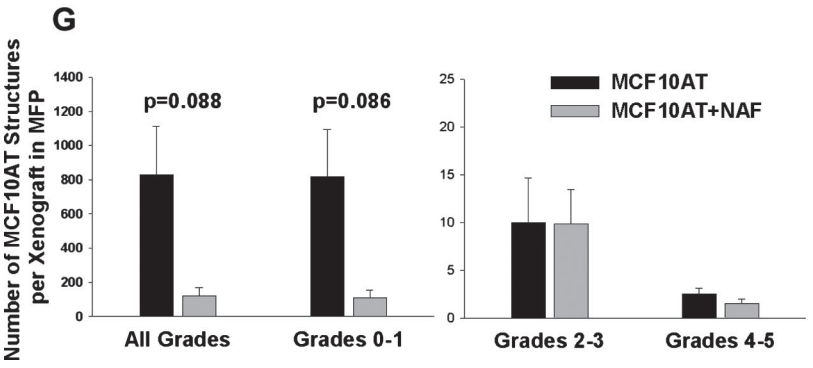

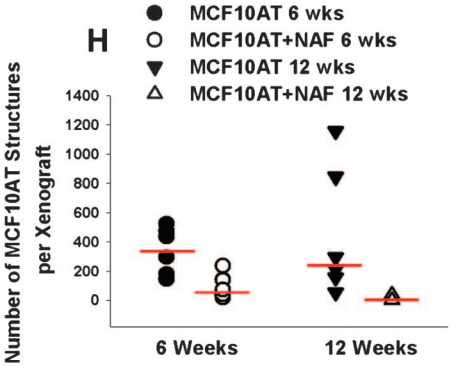

ing for Ki-67 and cleaved, activated caspase-3 was performed on xenografts with adequate tissue available. Overall, there was no significant difference in the rates of proliferation in MCF10AT xenografts versus MCF10AT + NAF xenografts of grade 0 to 1 (mean, 17.8 and 16.8% Ki-67 labeling, respectively) and grade 4 to 5 structures (13.8 and 11.1% Ki-67 labeling, respectively) (Figure 2E). However, NAF1 induced a statistically significant 2.4-fold decrease ($P < 0.001$) in Ki-67 labeling in grade 0 to 1 structures, whereas, NAF2 and NAF3 induced a 1.1- and 1.7-fold increase in proliferation (data not shown). Overall, apoptosis of MCF10AT cells in grade 0 to 1 structures was significantly increased by NAFs (mean, 0.5 and 3.1% cleaved caspase-3 labeling in MCF10AT xenografts and MCF10AT + NAF xenografts, respectively; $P = 0.019$) (Figure 2F). All three NAFs induced an increase in apoptosis of grade 0 to 1 structures. There was no difference in the rates of apoptosis in grade 4 to 5 structures in MCF10AT xenografts versus MCF10AT + NAF xenografts (Figure 2F). In sum, these results indicate that the presence of NAFs inhibited the growth of grade 0 to 1 MCF10AT structures, corresponding to normal and mildly hyperplastic ducts, whereas, grade 4 to 5 structures, corresponding to *in situ* and invasive carcinoma, were relatively resistant to growth inhibition by NAF. The inhibitory capacity of NAF, for both grade 0 to 1 and grade 4 to 5 structures, varied among NAF from different individuals. The growth inhibition appears to be mediated primarily by an increase in apoptosis.

In addition to performing subcutaneous xenografts, a subset of xenografts (MCF10AT and MCF10AT + NAF2) was prepared in the mammary fat pad and allowed to grow for 6 weeks. These orthotopic xenografts exhibited the same variety of histological grades of MCF10AT structures observed in the subcutaneous xenografts and differed only in the lower take of MCF10AT xenografts (50%) in comparison to subcutaneous MCF10AT xenografts (95%) at 6 weeks. The viability of orthotopic MCF10AT + NAF xenografts (100%) was similar to subcutaneous MCF10AT + NAF xenografts (92%) prepared using the same NAF culture (ie, NAF2). Similar to subcutaneous xenografts, the MCF10AT + NAF xenografts in the mammary fat pad ($n = 8$) exhibited a reduction in the number of epithelial structures of all grades (mean, 120; P value = 0.088) and grade 0 to 1 (mean, 108; $P = 0.086$) (Figure 2G) compared with MCF10AT xenografts ($n = 4$) (all grades mean = 830, grade 0 to 1 mean = 818), although this difference did not reach statistical significance because of the small sample size. There was no difference in the number of grade 2 to 3 or grade 4 to 5 epithelial structures in MCF10AT and MCF10AT + NAF xenografts located in the mammary fat pad (Figure 2G). These results mirror those for all subcutaneous xenografts (Figure 2, compare D and G).

To examine the effect of time on the growth of epithelial structures, a subset of subcutaneous xenografts (MCF10AT and MCF10AT + NAF1 xenografts) was allowed to grow for 12 weeks. The reduction in the mean number of epithelial cell structures in MCF10AT + NAF xenografts was greater at 12 weeks than 6 weeks ($P < 0.001$) (Figure 2H). Three of eight MCF10AT + NAF xenografts at 12 weeks were devoid of epithelial structures, and an additional three xenografts contained only one to three epithelial structures on histological evaluation of the thoroughly sectioned xenografts. In those MCF10AT + NAF xenografts without any residual MCF10AT epithelial cells, NAFs were also absent as indicated by T-FISH. In these cases, the presence of a xenograft was marked by organized ECM (ie, Matrigel), both grossly and microscopically. In contrast to MCF10AT + NAF xenografts, the number of epithelial structures in MCF10AT xenografts continued to rise throughout 12 weeks (Figure 2H).

NAFs Altered the Morphology of High-Grade Epithelial Structures

The presence of NAFs also led to morphological changes in grade 4 to 5 MCF10AT structures. In MCF10AT xenografts, the epithelial structures consisted of rounded groups of cohesive epithelial cells (Figure 3A), whereas in MCF10AT + NAF xenografts the structures had irregular borders, and the individual cells were more elongated and slightly less cohesive (Figure 3B). This morphological change was consistent with epithelial to mesenchymal transition (EMT), which was supported by a concomitant increase in vimentin expression in MCF10AT cells in grade 4 to 5 structures (Figure 3, A and B). The mean immunoscore for vimentin was 1.04 ($n = 5$) in MCF10AT xenografts versus 1.97 ($n = 11$) in MCF10AT + NAF xenografts ($P < 0.01$). Human-specific vimentin staining also confirmed the presence of individual human

Figure 2. The presence of NAFs decreases the growth of MCF10AT cells in MCF10AT + NAF xenografts. **A:** H&E stain of nine histological grade 0 structures and one grade 2 structure in a MCF10AT xenograft. Each MCF10AT structure is outlined. Only structures sufficiently cut through for evaluation were counted. Grade 0 to 1 structures were identified by their small size and/or the presence of one to three cell layers. The grade 2 structure consists of an enlarged duct with luminal bridging by epithelial cells. **B:** H&E stain of a histological grade 4 structure (outlined) in an MCF10AT xenograft surrounded by five grade 0 to 1 structures. Duct distension, rounded lumens, and enlarged nuclei characterize the grade 4 structure. **C:** H&E stain of one grade 5 and two grade 3 structures (outlined) in a MCF10AT + NAF xenograft. The grade 3 structures have a micropapillary configuration and the grade 5 structure consists of invasive epithelial cells with enlarged nuclei and prominent nucleoli. **D:** MCF10AT + NAF subcutaneous xenografts ($n = 22$) contained significantly fewer epithelial structures of all histological grades and grade 0 to 1 than MCF10AT xenografts ($n = 21$). There was no significant difference in the number of histological grade 2 to 3 and 4 to 5 structures in MCF10AT + NAF versus MCF10AT xenografts. **E:** The percentage of Ki-67-positive MCF10AT epithelial cells comprising grade 0 to 1 structures was not significantly different in subcutaneous MCF10AT xenografts ($n = 21$) versus MCF10AT + NAF xenografts ($n = 19$). Likewise, there was not significant difference in Ki-67 labeling in grade 4 to 5 structures in MCF10AT xenografts ($n = 13$) and MCF10AT + NAF xenografts ($n = 11$). **F:** The percentage of MCF10AT cells positive for cleaved caspase-3 in grade 0 to 1 structures was significantly higher in MCF10AT + NAF xenografts ($n = 11$) versus MCF10AT xenografts ($n = 15$). There was no statistically significant difference in the number of MCF10AT cells positive for cleaved caspase-3 in grade 4 to 5 structures in MCF10AT ($n = 9$) versus MCF10AT + NAF ($n = 6$) xenografts. **G:** When placed in the mammary fat pad (MFP), MCF10AT + NAF xenografts ($n = 8$) contained fewer epithelial structures of all histological grades and grade 0 to 1 than MCF10AT xenografts ($n = 4$), although this decrease did not reach statistical significance. There was no difference in the number of histological grade 2 to 3 and 4 to 5 structures in MCF10AT versus MCF10AT + NAF xenografts. **H:** The number of epithelial structures was significantly lower in MCF10AT + NAF xenografts at 12 weeks ($n = 8$) than 6 weeks ($n = 8$) ($P < 0.001$). For statistical analysis, the data were subjected to log transformation because of heterogeneity of variance, and the bars represent medians. Original magnifications, ×200 (**A–C**).

Table 3. Fold Decrease in the Number of MCF10AT Structures in Subcutaneous MCF10AT + NAF Xenografts Containing NAF1, NAF2, or NAF3

	Number of structures							
	All grades		Grades 0 to 1		Grades 2 to 3		Grades 4 to 5	
	Fold decrease	*P* value*	Fold decrease	*P* value	Fold decrease	*P* value	Fold decrease	*P* value
MCF10AT + NAF1	4.7	$P < \mathbf{0.001}$	4.8	$P < \mathbf{0.001}$	3.5	$P < \mathbf{0.001}$	0.7	$P = 0.317$
MCF10AT + NAF2	1.3	$P = 0.322$	1.4	$P = 0.270$	0.5	$P = 0.251$	0.7	$P = 0.258$
MCF10AT + NAF3	2.1	$P = 0.071$	2.2	$P = \mathbf{0.044}$	0.5	$P = 0.377$	∞	$P < \mathbf{0.001}$

*Bold face type indicates statistical significance, and italicized type indicates borderline statistical significance.

fibroblasts within ECM of MCF10AT + NAF xenografts. However, immunostaining of MCF10AT cells for E-cadherin failed to detect a decrease in its membrane expression in grade 4 to 5 structures in MCF10AT + NAF xenografts (mean immunoscore = 0.29) compared with MCF10AT xenografts (mean immunoscore = 0.27; *P* value = 0.81), as is characteristic of EMT.[26] Instead, we noted a significant increase in cytoplasmic E-cadherin expression in MCF10AT + NAF xenografts (mean immunoscore = 1.16) versus MCF10AT xenografts (mean immunoscore = 0.46) ($P = 0.017$) (Figure 3, C and D).

The Xenograft Stroma Is Altered by the Presence of NAFs in MCF10AT + NAF Xenografts

ECM Changes

In MCF10AT xenografts, the ECM had a homogeneous texture and coloration on H&E-stained sections (Figure 3E), whereas it consisted of lighter and darker areas in MCF10AT + NAF xenografts, suggesting differences in ECM composition (Figure 3F). To further characterize the ECM produced by NAFs in NAF xenografts and MCF10AT + NAF xenografts, fibulin 1, an ECM glycoprotein involved in laminin polymerization, was detected by immunohistochemistry with an antibody specific for the human form of fibulin 1. NAF xenografts and MCF10AT + NAF xenografts exhibited positive staining for fibulin 1 in the ECM (Figure 3H), whereas MCF10AT xenografts (Figure 3G) lacked positivity. These results suggested that NAFs humanized the xenograft ECM by producing human cell-derived ECM proteins, such as fibulin 1.

MVD Count

Murine vasculature was observed in the stroma of the xenografts. Angiogenesis was assessed in a subset of xenografts (MCF10AT and MCF10AT + NAF1 xenografts) grown for 6 weeks. Xenografts were stained with anti-von Willebrand factor (Figure 3, I and J), and MVD was determined. MCF10AT + NAF xenografts had a significantly higher number of new vessels ($n = 7$, mean MVD = 10.55) compared with MCF10AT xenografts ($n = 6$, mean MVD = 4.25) ($P = 0.008$) (Figure 3K). The mean MVD for NAF xenografts, which were those xenografts containing only NAF1 without MCF10AT cells, was 9.5 and was similar to that of MCF10AT + NAF xenografts.

Inflammatory Infiltrate

On routine histological examination, the presence of an inflammatory infiltrate in both MCF10AT xenografts and MCF10AT + NAF xenografts was observed. Multinucleated giant cells (foreign body type) were observed at each time point and in each group, whereas polymorphonuclear cells occurred infrequently and only in MCF10AT + NAF xenografts. Lymphocytes were the predominant cell type in the inflammatory infiltrate in both MCF10AT and MCF10AT + NAF xenografts. NAF xenografts exhibited very minimal or no lymphocytic infiltrate.

The intensity of the lymphocytic infiltrate was categorized as 0, +, ++, or +++. An absence of lymphocytic infiltration was scored as 0, whereas the highest level of infiltration was scored as +++ (Figure 4C). A low level of infiltration was scored as + (Figure 4A) and a medium level as ++ (Figure 4B). Scores 0 and + constituted the majority of MCF10AT xenografts, and scores ++ and +++ prevailed in MCF10AT + NAF xenografts indicating a lower level of lymphocytic infiltration in MCF10AT xenografts than in MCF10AT + NAF xenografts (Figure 4D). When examining the location of lymphocytes in xenografts, the highest concentration was found adjacent to the grade 4 to 5 structures (ie, ductal carcinoma *in situ* and invasive carcinoma).

To characterize further the type of lymphocytes present, the xenografts were stained immunohistochemically with anti-B220 antibody to detect B cells (Figure 4E) and anti-CD3 antibody to mark T cells (Figure 4F). CD3 is present primarily in mature T cells; however, it has also been detected in a population of T-cell progenitors (pre-T cells).[27] CD3-, CD4-, and CD8-positive T cells have been identified in low numbers in athymic mice,[28] and there are reports of extra-thymic maturation of T cells.[28,29] As expected, infiltration by CD3-positive lymphocytes was overall lower than B220-positive, B-cell infiltration.

Discussion

Human breast fibroblasts were successfully incorporated into the MCF10AT xenograft model of proliferative breast disease and persisted within MCF10AT + NAF xenografts for 12 weeks and in NAF xenografts for 20 weeks. Detection of the human fibroblasts in the xenografts was accomplished using CMFDA and human genomic T-FISH. Persistence of CMFDA was limited to 3 weeks, after which the tracker was no longer detectable intracel-

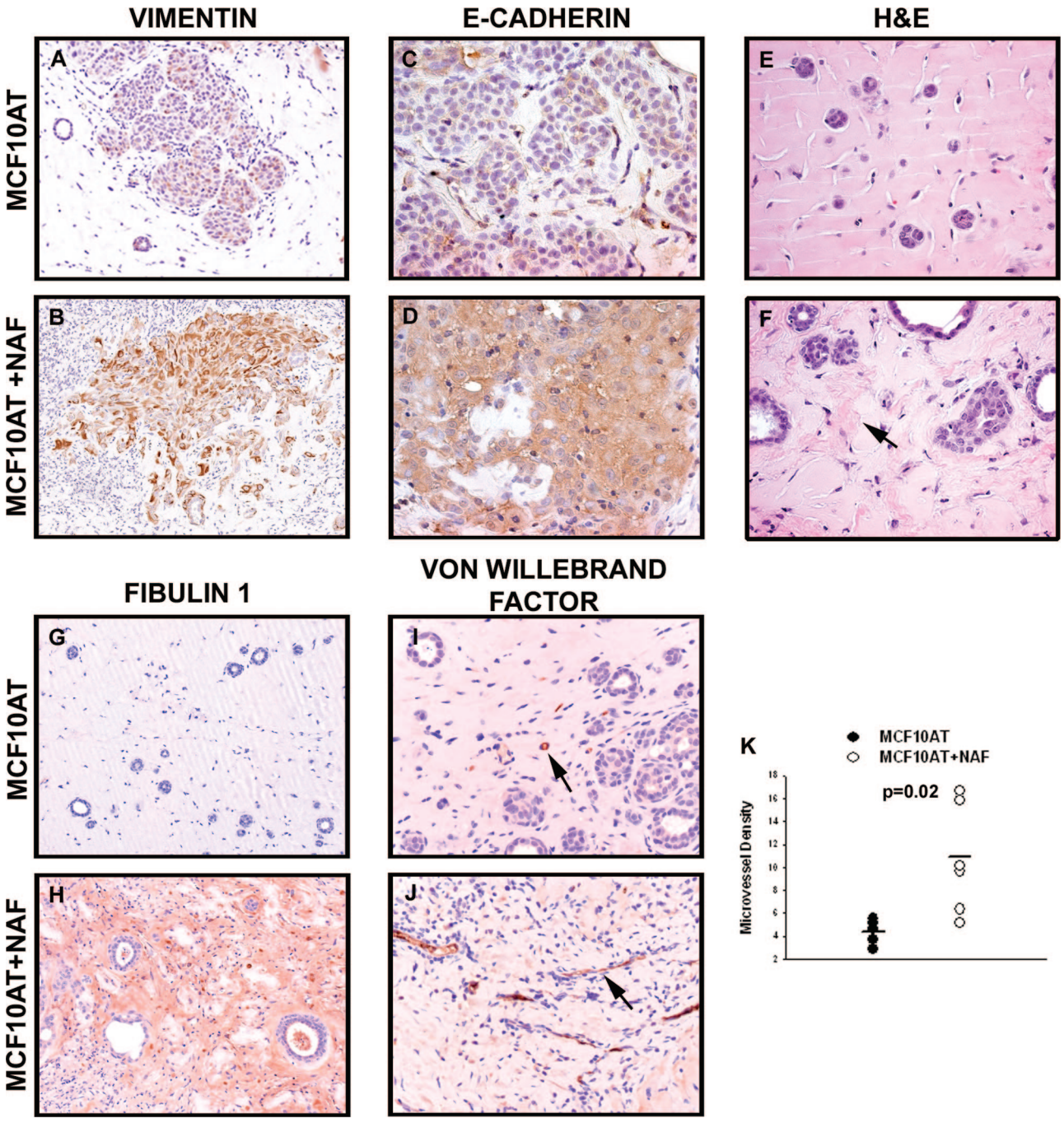

Figure 3. Epithelial and stromal changes observed in MCF10AT + NAF xenografts. **A** and **B:** A histological grade 5 structure in a MCF10AT xenograft was composed of rounded groups of tightly cohesive epithelial cells (**A**), whereas a grade 5 structure in a MCF10AT + NAF xenograft had irregular borders and elongate epithelial cells with reduced cohesion (**B**). Coincidentally, vimentin expression (brown staining) was also increased in epithelial cells in MCF10AT + NAF xenografts (**B**) compared with MCF10AT xenografts (**A**). **C** and **D:** Immunostaining for E-cadherin (brown staining) in grade 5 structures in MCF10AT cells was lower in MCF10AT xenografts (**C**) compared with MCF10AT + NAF xenografts (**D**). **E** and **F:** The ECM in MCF10AT xenografts was more homogeneous in coloration on H&E staining (**E**) than the ECM in MCF10AT + NAF xenografts (**F**), which had two-toned appearance (**arrows**), suggesting altered ECM composition. **G** and **H:** Immunostaining for human fibulin 1 (brown staining) was found in ECM and fibroblasts in MCF10AT + NAF xenografts (**H**) but was absent in MCF10AT xenografts (**G**). **I** and **J:** In comparison to MCF10AT xenografts (**I**), vessel formation (**arrows**) was increased in MCF10AT + NAF xenografts (**J**) as demonstrated by immunostaining for von Willebrand factor. **K:** The MVD count was increased in MCF10AT + NAF xenografts ($n = 7$, mean MVD = 10.55) versus MCF10AT xenografts ($n = 6$, MVD = 4.25) ($P = 0.008$, *t*-test). Original magnifications: ×200 (**A**, **B**, **G**, **H**); ×400 (**C–F**, **I**, **J**).

lularly. Presumably, the labeled cells had divided and diminished the intracellular concentration to undetectable levels. Genomic T-FISH established the presence of fibroblasts in 6- and 12-week MCF10AT + NAF xenografts.

NAFs in MCF10AT + NAF xenografts inhibited the growth of MCF10AT epithelial cells as demonstrated by an overall decrease in the number of MCF10AT structures. However, NAFs reduced the number of histological grade 0 to 1 MCF10AT structures preferentially. This

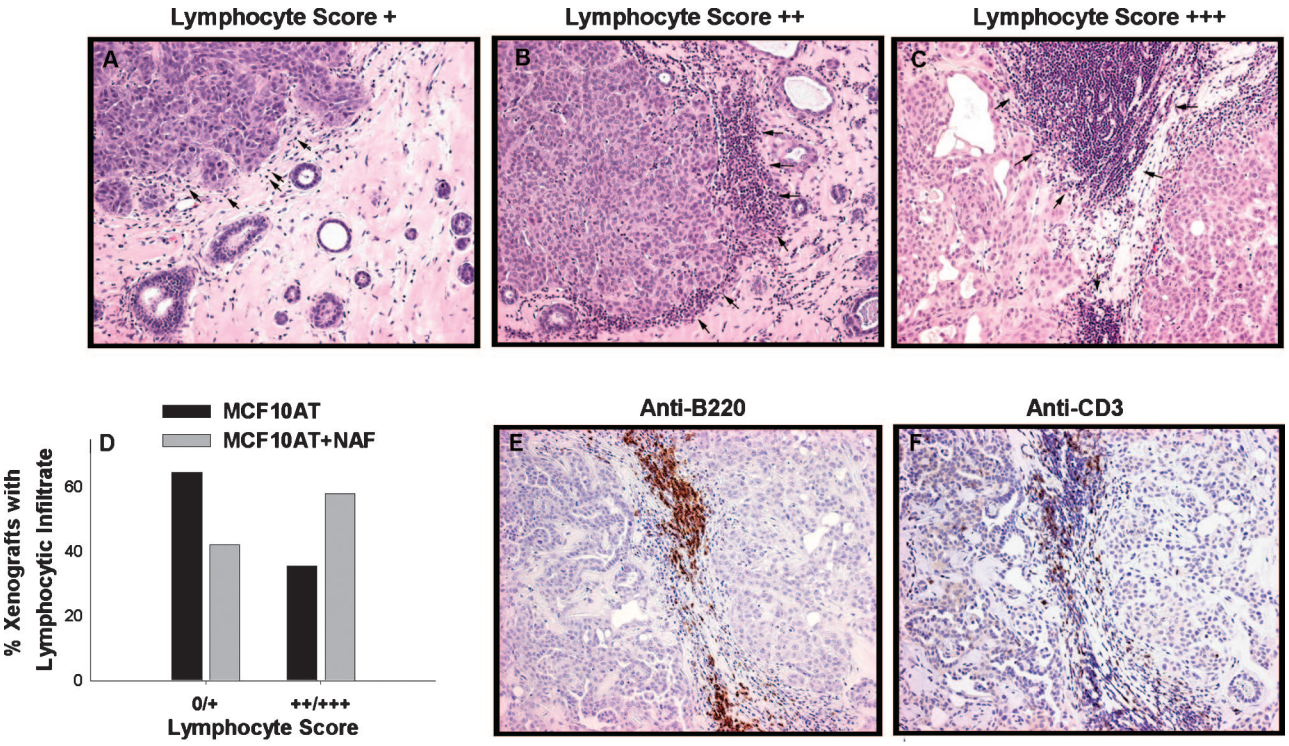

Figure 4. Lymphocytic infiltration differs in MCF10AT xenografts and MCF10AT + NAF xenografts. **A:** A lymphocytic score of + represented few scattered lymphocytes that occasionally formed small clusters. **B:** A lymphocytic score of ++ indicated a moderate number of lymphocytes that readily formed aggregates. **C:** A lymphocyte score of +++ depicted the highest number of lymphocytes that form large aggregates. **D:** A higher level of lymphocytic infiltrate (++/+++) was present more frequently in MCF10AT + NAF xenografts than MCF10AT xenografts. **E:** B-cell infiltration into xenografts was demonstrated by immunostaining for anti-B220, which marked a majority of cells in the lymphocytic infiltrate. **F:** Immunostaining with the anti-CD3 antibody marked T cells. The number of T cells was much less than B cells. Original magnifications, ×200.

reduction appeared to be mediated primarily by enhanced apoptosis. Overall, the presence of NAFs suppressed the growth of MCF10AT cells with a normal or mildly hyperplastic phenotype, which constitutes grade 0 to 1 structures, but had less affect on the growth of the more transformed epithelial cells that form higher grade structures, corresponding to ductal carcinoma *in situ* and invasive carcinoma. This suggests that as neoplastic transformation progresses, epithelial cells become increasingly resistant to growth regulation by NAF. On the other hand, the presence of the more transformed, high-grade lesions may have altered surrounding NAF, via cross-talk between NAFs and epithelial cells, rendering them less able to inhibit epithelial cell growth. However, any change induced in the NAFs was insufficient to significantly promote the growth of the high-grade lesions, as has been reported for CAFs.[7] All three NAFs reduced the number of grade 0 to 1 structures to some degree, but there was variation in the growth inhibitory capacity of NAFs from different individuals, as has been reported previously.[7,12]

A previous study demonstrated that NAFs regulate the growth of normal human breast epithelial cells in engraftments of fibroblasts with epithelial organoids, both derived from breast reduction specimens, in humanized mouse mammary fat pads. Mammary fat pads were humanized by injection with immortalized and irradiated NAFs. After humanization, NAFs were co-engrafted with the breast epithelial cells and allowed to grow for 8 weeks. NAFs suppressed formation of hyperplastic lesions, which otherwise occurred in the absence of NAFs.[30] In another study, NAFs were unable to inhibit growth of MCF7 breast carcinoma cells carrying an activated *ras* oncogene.[7] In contrast, CAFs promoted the growth of the MCF7 xenografts.[7] Multiple studies have demonstrated that CAFs have a stronger growth-promoting effect on normal or cancerous breast epithelial cells than NAFs.[31–36] Overall, these previous results support our findings indicating that NAFs inhibit the growth of normal or hyperplastic epithelium, but are, in general, less able to alter the growth of cancer epithelial cells.

The presence of NAFs also affected the phenotype of the MCF10AT cells in the grade 4 to 5 structures, corresponding to ductal carcinoma *in situ* and invasive carcinoma. The MCF10AT cells constituting these structures were more elongate and demonstrated some loss of cohesion. In addition, expression of vimentin in the epithelial cells was increased. These changes suggest induction of EMT; however, this was not confirmed by decreased membrane expression of E-cadherin.[26] This phenotypic alteration in high-grade lesions in MCF10AT + NAF xenografts may have contributed to their resistance to growth inhibition by some NAFs and their ability to persist.

The presence of human NAFs also induced changes in the xenograft stroma, including the ECM, vasculature, and inflammatory infiltrate. The molecular mechanisms underlying the NAF-induced changes in the number of MCF10AT structures and their phenotype remain to be

elucidated but may include direct paracrine signaling between fibroblasts and epithelial cells or interactions between fibroblasts and other stromal components. NAFs humanized the ECM in MCF10AT + NAF xenografts and NAF xenografts by secreting human ECM proteins as demonstrated by the presence of human fibulin 1. Both tumor suppressive and tumor promoting activities have been reported for fibulin 1, depending on the isoform of the protein being expressed.[37–39] Fibulin 1 expression in breast cancers is also immunogenic, eliciting both an antibody response and a T-cell-mediated response.[40] Therefore, fibulin 1 may have played a role in attracting lymphocytes to MCF10AT + NAF xenografts or may have directly inhibited growth of lower grade structures. The former possibility is less likely given that human fibulin 1 was detected in xenografts containing NAFs only, but these NAF xenografts did not attract lymphocytes.

Fibroblasts secrete growth factors and chemokines (eg, basic fibroblast growth factor, vascular endothelial growth factor, platelet-derived growth factor, stromal-derived factor-1) that have been implicated in the recruitment of endothelial cells either directly or indirectly through activation of inflammatory cells.[4,7,41] Therefore, the enhanced angiogenesis observed in the MCF10AT + NAF xenografts is not surprising. Neoangiogenesis induced by cancer enhances tumor progression.[7] The increase in angiogenesis in MCF10AT + NAF xenografts did not coincide with overall MCF10AT growth but may have played a role in the persistence of higher grade lesions and/or in the increased inflammatory infiltrate (by providing additional channels for lymphocyte access).

The lymphocytic infiltrate in MCF10AT + NAF xenografts was predominantly composed of B cells. Although an anti-tumor role for T cells is established,[42] the role of B cells and humoral immunity in cancer is controversial. Some studies have demonstrated a tumor suppressive function for B cells or humoral immunity stimulated by tumor-associated antigens,[38,43] whereas others report a promotional role for B cells in carcinogenesis.[44] Either the presence of fibroblasts or, more likely, the interactions of NAFs with MCF10AT cells attracted lymphocytes to a greater extent than MCF10AT cells alone. Fibroblasts can be induced to secrete inflammatory cytokines[45] and are known to regulate the composition and function of recruited lymphocytes.[46] The lymphocytic infiltrate induced by the presence of NAFs may have contributed to the decrease in both MCF10AT cells and NAFs in MCF10AT + NAF xenografts.

This study established that NAFs inhibited the growth of MCF10AT epithelial cells *in vivo*, but the magnitude of this inhibition was dependent on the phenotypes of the MCF10AT cells (ie, the histological grade of the MCF10AT structures) and the NAFs (ie, interindividual variation among NAF). In general, the results suggest that NAFs exert the greatest inhibition against normal and hyperplastic epithelium. Therefore, potential therapeutic strategies of normalizing the stroma surrounding *in situ* proliferative lesions and cancer may be particularly effective if applied early in cancer progression.

Acknowledgments

We thank Gregg G. Magrane, Ph.D., University of California, San Francisco, CA, for technical consultation on genomic hybridization; Cynthia Moore and Cecil R. Stockard for assistance with immunohistochemical staining; Denise R. Shaw, Ph.D., for consultation on the immunology of nude mice; Denise K. Oelschlager for technical assistance with xenograft preparation; the High Resolution Imaging Facility at the University of Alabama at Birmingham, Birmingham, AL, for technical assistance with imaging; and Richard D. Lopez, M.D., for careful and insightful review of the manuscript.

References

1. Kurose K, Gilley K, Matsumoto S, Watson PH, Zhou XP, Eng C: Frequent somatic mutations in PTEN and TP53 are mutually exclusive in the stroma of breast carcinomas. Nat Genet 2002, 32:355–357
2. Kurose K, Hoshaw-Woodard S, Adeyinka A, Lemeshow S, Watson PH, Eng C: Genetic model of multi-step breast carcinogenesis involving the epithelium and stroma: clues to tumour-microenvironment interactions. Hum Mol Genet 2001, 10:1907–1913
3. Liotta LA, Kohn EC: The microenvironment of the tumour-host interface. Nature 2001, 411:375–379
4. Mueller MM, Fusenig NE: Friends or foes—bipolar effects of the tumour stroma in cancer. Nat Rev Cancer 2004, 4:839–849
5. Bhowmick NA, Neilson EG, Moses HL: Stromal fibroblasts in cancer initiation and progression. Nature 2004, 432:332–337
6. Horgan K, Jones DL, Mansel RE: Mitogenicity of human fibroblasts in vivo for human breast cancer cells. Br J Surg 1987, 74:227–229
7. Orimo A, Gupta PB, Sgroi DC, Arenzana-Seisdedos F, Delaunay T, Naeem R, Carey VJ, Richardson AL, Weinberg RA: Stromal fibroblasts present in invasive human breast carcinomas promote tumor growth and angiogenesis through elevated SDF-1/CXCL12 secretion. Cell 2005, 121:335–348
8. Moinfar F, Man YG, Arnould L, Bratthauer GL, Ratschek M, Tavassoli FA: Concurrent and independent genetic alterations in the stromal and epithelial cells of mammary carcinoma: implications for tumorigenesis. Cancer Res 2000, 60:2562–2566
9. Kunz-Schughart LA, Knuechel R: Tumor-associated fibroblasts (part II): functional impact on tumor tissue. Histol Histopathol 2002, 17:623–637
10. Kunz-Schughart LA, Knuechel R: Tumor-associated fibroblasts (part I): active stromal participants in tumor development and progression? Histol Histopathol 2002, 17:599–621
11. Tlsty TD: Stromal cells can contribute oncogenic signals. Semin Cancer Biol 2001, 11:97–104
12. Sadlonova A, Novak Z, Johnson MR, Bowe DB, Gault SR, Page GP, Thottassery JV, Welch DR, Frost AR: Breast fibroblasts modulate epithelial cell proliferation in three-dimensional in vitro co-culture. Breast Cancer Res 2005, 7:R46–R59
13. Cullen KJ, Smith HS, Hill S, Rosen N, Lippman ME: Growth factor messenger RNA expression by human breast fibroblasts from benign and malignant lesions. Cancer Res 1991, 51:4978–4985
14. Heffelfinger SC, Miller MA, Yassin R, Gear R: Angiogenic growth factors in preinvasive breast disease. Clin Cancer Res 1999, 5:2867–2876
15. Ito A, Nakajima S, Sasaguri Y, Nagase H, Mori Y: Co-culture of human breast adenocarcinoma MCF-7 cells and human dermal fibroblasts enhances the production of matrix metalloproteinases 1, 2 and 3 in fibroblasts. Br J Cancer 1995, 71:1039–1045
16. Brummer O, Athar S, Riethdorf L, Loning T, Herbst H: Matrix-metalloproteinases 1, 2, and 3 and their tissue inhibitors 1 and 2 in benign and malignant breast lesions: an in situ hybridization study. Virchows Arch 1999, 435:566–573
17. Soule HD, Maloney TM, Wolman SR, Peterson Jr WD, Brenz R, McGrath CM, Russo J, Pauley RJ, Jones RF, Brooks SC: Isolation and characterization of a spontaneously immortalized human breast epithelial cell line, MCF-10. Cancer Res 1990, 50:6075–6086

18. Heppner GH, Wolman SR: MCF-10AT: a model for human breast cancer development. Breast J 1999, 5:122–129
19. Dawson PJ, Wolman SR, Tait L, Heppner GH, Miller FR: MCF10AT: a model for the evolution of cancer from proliferative breast disease. Am J Pathol 1996, 148:313–319
20. Miller FR, Soule HD, Tait L, Pauley RJ, Wolman SR, Dawson PJ, Heppner GH: Xenograft model of progressive human proliferative breast disease. J Natl Cancer Inst 1993, 85:1725–1732
21. Shekhar MP, Werdell J, Santner SJ, Pauley RJ, Tait L: Breast stroma plays a dominant regulatory role in breast epithelial growth and differentiation: implications for tumor development and progression. Cancer Res 2001, 61:1320–1326
22. Weidner N, Folkman J, Pozza F, Bevilacqua P, Allred EN, Moore DH, Meli S, Gasparini G: Tumor angiogenesis: a new significant and independent prognostic indicator in early-stage breast carcinoma. J Natl Cancer Inst 1992, 84:1875–1887
23. Frost AR, Sparks D, Grizzle WE: Methods of antigen recovery vary in their usefulness in unmasking specific antigens in immunohistochemistry. Appl Immunohistochem Mol Morphol 2000, 8:236–243
24. Talley LI, Grizzle WE, Waterbor JW, Brown D, Weiss H, Frost AR: Hormone receptors and proliferation in breast carcinomas of equivalent histologic grades in pre- and postmenopausal women. Int J Cancer 2002, 98:118–127
25. Kubitz R, Warskulat U, Schmitt M, Haussinger D: Dexamethasone- and osmolarity-dependent expression of the multidrug-resistance protein 2 in cultured rat hepatocytes. Biochem J 1999, 340:585–591
26. Cowin P, Rowlands TM, Hatsell SJ: Cadherins and catenins in breast cancer. Curr Opin Cell Biol 2005, 17:499–508
27. Ceredig R, Rolink T: A positive look at double-negative thymocytes. Nat Rev Immunol 2002, 2:888–897
28. Hardy B, Morgenstern S, Raiter A, Rodionov G, Fadaeev L, Niv Y: BAT monoclonal antibody immunotherapy of human metastatic colorectal carcinoma in mice. Cancer Lett 2005, 229:217–222
29. García-Ojeda ME, Dejbakhsh-Jones S, Chatterjea-Matthes D, Mukhopadhyay A, BitMansour A, Weissman IL, Brown JM, Strober S: Stepwise development of committed progenitors in the bone marrow that generate functional T cells in the absence of the thymus. J Immunol 2005, 175:4363–4373
30. Kuperwasser C, Chavarria T, Wu M, Magrane G, Gray JW, Carey L, Richardson A, Weinberg RA: Reconstruction of functionally normal and malignant human breast tissues in mice. Proc Natl Acad Sci USA 2004, 101:4966–4971
31. Gache C, Berthois Y, Martin PM, Saez S: Positive regulation of normal and tumoral mammary epithelial cell proliferation by fibroblasts in coculture. In Vitro Cell Dev Biol Anim 1998, 34:347–351
32. van Roozendaal CE, van Ooijen B, Klijn JG, Claassen C, Eggermont AM, Henzen-Logmans SC, Foekens JA: Stromal influences on breast cancer cell growth. Br J Cancer 1992, 65:77–81
33. van Roozendaal KE, Klijn JG, van Ooijen B, Claassen C, Eggermont AM, Henzen-Logmans SC, Foekens JA: Differential regulation of breast tumor cell proliferation by stromal fibroblasts of various breast tissue sources. Int J Cancer 1996, 65:120–125
34. Brouty-Boyé D, Mainguene C, Magnien V, Israel L, Beaupain R: Fibroblast-mediated differentiation in human breast carcinoma cells (MCF-7) grown as nodules in vitro. Int J Cancer 1994, 56:731–735
35. Gache C, Berthois Y, Cvitkovic E, Martin PM, Saez S: Differential regulation of normal and tumoral breast epithelial cell growth by fibroblasts and 1,25-dihydroxyvitamin D3. Breast Cancer Res Treat 1999, 55:29–39
36. Ryan MC, Orr DJ, Horgan K: Fibroblast stimulation of breast cancer cell growth in a serum-free system. Br J Cancer 1993, 67:1268–1273
37. Gallagher WM, Currid CA, Whelan LC: Fibulins and cancer: friend or foe? Trends Mol Med 2005, 11:336–340
38. Coronella-Wood JA, Hersh EM: Naturally occurring B-cell responses to breast cancer. Cancer Immunol Immunother 2003, 52:715–738
39. Forti S, Scanlan MJ, Invernizzi A, Castiglioni F, Pupa S, Agresti R, Fontanelli R, Morelli D, Old LJ, Pupa SM, Menard S: Identification of breast cancer-restricted antigens by antibody screening of SKBR3 cDNA library using a preselected patient's serum. Breast Cancer Res Treat 2002, 73:245–256
40. Pupa SM, Argraves WS, Forti S, Casalini P, Berno V, Agresti R, Aiello P, Invernizzi A, Baldassari P, Twal WO, Mortarini R, Anichini A, Menard S: Immunological and pathobiological roles of fibulin-1 in breast cancer. Oncogene 2004, 23:2153–2160
41. Dranoff G: Cytokines in cancer pathogenesis and cancer therapy. Nat Rev Cancer 2004, 4:11–22
42. Zou W: Immunosuppressive networks in the tumour environment and their therapeutic relevance. Nat Rev Cancer 2005, 5:263–274
43. Quan N, Zhang Z, Demetrikopoulos MK, Kitson RP, Chambers WH, Goldfarb RH, Weiss JM: Evidence for involvement of B lymphocytes in the surveillance of lung metastasis in the rat. Cancer Res 1999, 59:1080–1089
44. de Visser KE, Korets LV, Coussens LM: De novo carcinogenesis promoted by chronic inflammation is B lymphocyte dependent. Cancer Cell 2005, 7:411–423
45. Brouty-Boyé D, Pottin-Clemenceau C, Doucet C, Jasmin C, Azzarone B: Chemokines and CD40 expression in human fibroblasts. Eur J Immunol 2000, 30:914–919
46. Silzle T, Randolph GJ, Kreutz M, Kunz-Schughart LA: The fibroblast: sentinel cell and local immune modulator in tumor tissue. Int J Cancer 2004, 108:173–180